AD-A084 025   NAVAL POSTGRADUATE SCHOOL   MONTEREY CA   F/G 20/3
                   AN INVESTIGATION OF MAGNETO-ACOUSTIC EFFECTS IN CONDUCTIVE FLUI--ETC(U)
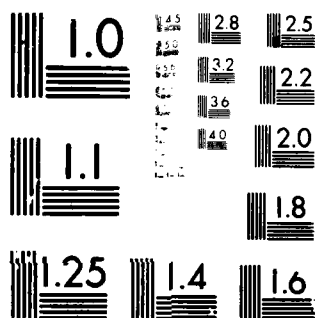   DEC 79   R F KLAUS
UNCLASSIFIED   NL

END
DATE
FILMED
6-80
DTIC

1.0

1.1

1.25

4.5
5.0

2.8

3.2

3.6

4.0

2.5

2.2

2.0

1.4

1.6

1.8

MICROCOPY RESOLUTION TEST CHART
NATIONAL BUREAU OF STANDARDS-1963-A

LEVEL

NAVAL POSTGRADUATE SCHOOL
Monterey, California

Master's THESIS

AN INVESTIGATION OF
MAGNETO-ACOUSTIC EFFECTS IN CONDUCTIVE FLUIDS.

by

Robert Franz/Klaus

Dec   79

Thesis Advisor: P.H. Moose

Approved for public release; distribution unlimited.

251 100

80   5   6 037

REPORT DOCUMENTATION PAGE		READ INSTRUCTIONS BEFORE COMPLETING FORM
1. REPORT NUMBER	2. GOVT ACCESSION NO. AD-A084025	3. RECIPIENT'S CATALOG NUMBER
4. TITLE (and Subtitle) An Investigation of Magneto-Acoustic Effects in Conductive Fluids		5. TYPE OF REPORT & PERIOD COVERED Master's Thesis; December 1979
		6. PERFORMING ORG. REPORT NUMBER
7. AUTHOR(s) Robert Franz Klaus		8. CONTRACT OR GRANT NUMBER(s)
9. PERFORMING ORGANIZATION NAME AND ADDRESS Naval Postgraduate School Monterey, California 93940		10. PROGRAM ELEMENT, PROJECT, TASK AREA & WORK UNIT NUMBERS
11. CONTROLLING OFFICE NAME AND ADDRESS Naval Postgraduate School Monterey, California 93940		12. REPORT DATE December 1979
		13. NUMBER OF PAGES 46
14. MONITORING AGENCY NAME & ADDRESS(If different from Controlling Office)		15. SECURITY CLASS. (of this report) Unclassified
		15a. DECLASSIFICATION/DOWNGRADING SCHEDULE

16. DISTRIBUTION STATEMENT (of this Report)

Approved for public release; distribution unlimited.

17. DISTRIBUTION STATEMENT (of the abstract entered in Block 20, if different from Report)

18. SUPPLEMENTARY NOTES

19. KEY WORDS (Continue on reverse side if necessary and identify by block number)

Magneto-acoustics

Sonomagnetic

20. ABSTRACT (Continue on reverse side if necessary and identify by block number)

An acoustic wave propagating in a conductive medium in the presence of a magnetic field will induce electric potential fields and currents, and, associated with the electric currents, secondary magnetic fields. This interaction is of interest because it occurs in acoustic propagation through sea water in the presence of the earth's magnetic field, and at ultra-low frequency (ULF), acoustic waves should be detectable. A Green's function solution in an

DD FORM 1473 EDITION OF 1 NOV 65 IS OBSOLETE
1 JAN 73
(Page 1)
S/N 0102-014-6601 |

#20 - ABSTRACT - CONTINUED

infinite medium is developed, with an infinite magnetic field
and an infinite plane acoustic wave, from which it can be seen
that the magneto-acoustic coupling strength varies linearly with
the strength of the acoustic wave and with the magnetic field,
and is inversely proportional to frequency. An experiment is
described and analyzed in which this interaction is verified for
a specific laboratory geometry to within an order of magnitude.
Possible sources of the discrepancy in the magnitude of the
effect are discussed, and some potential refinements for future
experimentation are also noted.

An Investigation of
Magneto-Acoustic Effects in Conductive Fluids

by

Robert Franz Klaus
Lieutenant, United States Navy
B.S., United States Naval Academy, 1973

Submitted in partial fulfillment of the
requirements for the degree of

MASTER OF SCIENCE IN ENGINEERING ACOUSTICS

from the

NAVAL POSTGRADUATE SCHOOL
December 1979

Author _____

Approved by: _____
                                        Thesis Advisor

_____
                                        Second Reader

_____
                     Chairman, Department of Physics

_____
                     Dean of Science and Engineering

3

ABSTRACT

An acoustic wave propagating in a conductive medium in the presence of a magnetic field will induce electric potential fields and currents, and, associated with the electric currents, secondary magnetic fields. This interaction is of interest because it occurs in acoustic propagation through sea water in the presence of the earth's magnetic field, and at ultra-low frequency (ULF), acoustic waves should be detectable. A Green's function solution in an infinite medium is developed, with an infinite magnetic field and an infinite plane acoustic wave, from which it can be seen that the magneto-acoustic coupling strength varies linearly with the strength of the acoustic wave and with the magnetic field, and is inversely proportional to frequency. An experiment is described and analyzed in which this interaction is verified for a specific laboratory geometry to within an order of magnitude. Possible sources of the discrepancy in the magnitude of the effect are discussed, and some potential refinements for future experimentation are also noted.

4

TABLE OF CONTENTS

LIST OF DRAWINGS

ACKNOWLEDGMENT

I. INTRODUCTION

It has been suggested by previous investigations that an acoustic wave propagating in a conductive medium in the presence of a strong magnetic field will induce electric fields. Further, these electric fields can generate magnetic waves due to their associated currents. These, in turn, are capable of interacting with the original acoustic wave.

In 1952, Anderson[1] analyzed longitudinal magneto-hydrodynamic effects. Sound waves propagating in a conductive medium will undergo a change in velocity due to the constraining forces acting on the fluid from the magnetic field. His paper developed a theoretical model for predicting the dispersion and absorption of the initiating acoustic wave in media of finite conductivity.[2]

After a long pause in the literature, Bird[3] wrote a paper in 1977 which investigated hydromagnetism from submerged acoustic sources. He introduced the term "sonomagnetic

---

[1]Neal S. Anderson, "Longitudinal Magneto-Hydrodynamic Waves," Journal of the Acoustical Society of America (JASA), May, 1953.

[2]Kornhauser ("Magnetic Damping of Acoustic Waves in Conducting Media," JASA, July, 1953) pointed out an unfortunate numerical error which invalidated the quantitative results of Anderson.

[3]J. F. Bird, "Hydromagnetism Induced by Submerged Acoustic Sources: Sonomagnetic Pseudoradiation," JASA, November, 1977.

pseudoradiation" to describe the effect; due to the characteristically weak nature of the induced magnetic fields, they do not propagate effectively of themselves, but are carried along by the propagating acoustic wave. The work develops in some detail a theoretical model for a semi-infinite conductive medium for several source geometries.

However, apparently these interactions have never been observed in a laboratory experiment. The objective of the research reported here has been to verify the existence of the magneto-acoustic effect and compare its strength with theoretical prediction.

The phenomenon is of interest for a variety of potential applications, some of which are noted here. There is a continuing interest in the attenuation of sound in seawater, especially at the lower frequencies. As will be observed later, the coupling of energy from the acoustic wave into an electromagnetic field is more pronounced at lower frequencies, and this interaction could possibly account for some acoustic attenuation.

Also of interest is the possibility that this phenomenon is a source of ultra-low frequency (ULF) noise in geomagnetic measurements at sea.

Another facet of interest is the potential use of this coupling effect as a means of observing low frequency acoustic waves by their electric or magnetic signatures. Since this effect is sensitive to the acoustic velocity field as a vectoral quantity, it provides directional information from a

point measurement. The possible benefits of observing ULF acoustic waves with an electromagnetic antenna, as opposed to large conventional acoustic arrays, are very appealing.

Before any of these postulated applications can be attempted, however, there is a need to experimentally verify the basic phenomenon of magneto-acoustic interactions. The objective of this thesis is to provide a preliminary verification of the existence of the coupling effect. To accomplish this, a general solution in an infinite medium is first examined, and then a laboratory experiment exploring the phenomenon is reported and discussed.

II. GENERAL THEORY

This section reviews and discusses a solution for an acoustic plane wave in an infinite medium, from which several significant characteristics of the interaction are evident.

First, consider a magnetic field of the form

$$\bar{B} = \bar{B}_o \, e^{i\omega t} \tag{1}$$

so that

$$\frac{\partial \bar{B}}{\partial t} = i\,\omega\,\bar{B} \tag{2}$$

Then, from Maxwell's equations, for a linear medium,

$$\nabla \times \bar{E} = -\,i\,\omega\,\bar{B} \tag{3}$$

and

$$\nabla \times \frac{\bar{B}}{\mu} = \bar{J} + \frac{\partial \bar{D}}{\partial t} \tag{4}$$

$\bar{J}$ is the normal current density, $\bar{D}$ is the displacement current, and μ is the permittivity. However, for frequencies less than about 10^9 Hz, the displacement current is negligible, so that

$$\nabla \times \frac{\overline{B}}{\mu} = \overline{J} = \overline{J}_o + \overline{J}_1 = \overline{J}_o + \sigma\overline{E} , \quad (5)$$

in the form of a source current and an induced current (σ is the conductivity of the solution). This can also be written

$$\nabla \times \overline{B} = \mu \overline{J}_o + \mu \sigma \overline{E} . \quad (6)$$

Taking the curl of both sides of equation (6) yields

$$- \nabla^2 \overline{B} = \mu \sigma(\nabla \times \overline{E}) + \mu(\nabla \times \overline{J}_o) ; \quad (7)$$

and combining equation (7) with equation (3) above results in

$$- \nabla^2 \overline{B} - \gamma^2 \overline{B} = - \mu(\nabla \times \overline{J}_o) , \quad (8)$$

where

$$\gamma = (i\omega\mu\sigma)^{1/2}$$

is the complex propagation constant. This is a standard wave equation in $\overline{B}$, the magnetic field strength.

Now introduce a plane acoustic wave propagating in the +z direction and assume a DC magnetic field, F, in the y-z plane, so that

$$F_y = F \sin \phi_f , \tag{9}$$

the magnetic field, and

$$\bar{V} = V_p \, e^{i(\omega t - kz)} \, \hat{k} , \tag{10}$$

the acoustic velocity field, are at right angles. k represents the acoustic wave number. The source current will then be

$$\bar{J}_o = \sigma \, \bar{V} \times \bar{F} , \tag{11}$$

or

$$J_{xo} = V_p \, F_y \, e^{i(\omega t - kz)} .$$

A Green's function method may be used to determine the effect that J_{xo} has on an arbitrary field point in spherical coordinates as follows. Define a vector potential $\bar{A}$ such that $\bar{B} = \Delta \times \bar{A}$. Then

$$\bar{A}(\bar{r}) = \frac{\mu}{4\pi} \int \bar{J}_o(\bar{r}') \, \frac{e^{-\gamma|\bar{r} - \bar{r}'|}}{|\bar{r} - \bar{r}'|} \, dv' \tag{12}$$

where

$$\frac{e^{-\gamma|\bar{r} - \bar{r}'|}}{|\bar{r} - \bar{r}'|}$$

is the Green's function solution for the wave equation defined in equation (8), $\bar{r}$ is the field position, and $\bar{r}'$ is the source point. Taking $\bar{r}$ to be zero (the origin of the coordinate system), and integrating over all space yields

$$A_x(0) = \frac{\mu}{\gamma^2 + k^2} \sigma V_p F_y e^{i\omega t} . \qquad (13)$$

Incorporating the propagation of the wave along the z-axis into this solution yields the vector potential components

$$A_x(z) = \frac{\mu}{\gamma^2 + k^2} \sigma V_p F_y e^{i(\omega t - kz)} \qquad (14)$$

and

$$A_y(z) = A_z(z) = 0 .$$

Then

$$\bar{B} = \nabla \times \bar{A} = B_y \hat{j} \qquad (15)$$

or

$$B_y = \frac{i\, k\, \mu\, \sigma}{\gamma^2 + k^2} V_p F_y e^{i(\omega t - kz)}$$

$$= \frac{\gamma^2}{\gamma^2 + k^2} \frac{V_p}{c} F_y e^{i(\omega t - kz)} \qquad (16)$$

14

where the acoustic wave number k has been taken as ω/c, with c the velocity of sound in the medium. Also,

$$B_x = B_z = 0 .$$

Eq. 16 gives a transverse propagating magnetic field induced by the propagating plane acoustic wave.

Two interesting factors appear in this equation: the first, $\frac{V_p}{c}$, is an acoustic mach number and introduces the magnitude of the acoustic wave into the output.

The second is the scaling factor,

$$\frac{\gamma^2}{\gamma^2 + k^2} .$$

In order to get a feeling for its effect, it is useful to introduce some approximations. First note the dependence on the conductivity and permittivity of the medium, and on the sound speed. For illustration, assume some typical values for these parameters from normal sea water and consider the frequency dependence of the scaling factor. If $\sigma = 4$ siemens/meter, $\mu = 4\pi \times 10^{-7}$ henries/meter, and $c = 1500$ meters/second, then

$$\frac{\gamma^2}{\gamma^2 + k^2} = \frac{i \omega \mu \sigma}{i \omega \mu \sigma + \dfrac{\omega^2}{c^2}} = \frac{i}{(8.84 \times 10^{-2})\omega + i}. \quad (17)$$

15

The magnitude of Eq. 17 is plotted against frequency in Figure (1).

Note that at low frequencies, it is approximately unity, but decreases sharply from about 1 Hz to about 50 Hz, falling off approximately as $1/\omega$. This illustrates that the magnitude of the energy coupling will only be appreciable at low frequencies in a real ocean environment and will be very small above 50 Hz.

Consider the overall effect of an actual ocean environment. The earth's magnetic field can be assumed to have a value of approximately $F = 5 \times 10^{-5}$ Tesla at mid-latitudes. For a plane acoustic wave with a pressure amplitude of 100 dB re 1 μPa, $V_p = 6.7 \times 10^{-8}$ meters/second. Incorporating these values into equation (16) gives

$$B_y (f = 1 \text{ Hz}) = 1.94 \times 10^{-15} e^{i(\omega t - kz)} \text{ Tesla,}$$

and

$$B_y (f = 100 \text{ Hz}) = 3.99 \times 10^{-17} e^{i(\omega t - kz)} \text{ Tesla.}$$

The decrease in coupling effect with frequency is readily apparent. Also, note Bird's[4] pseudoradiation effect: the
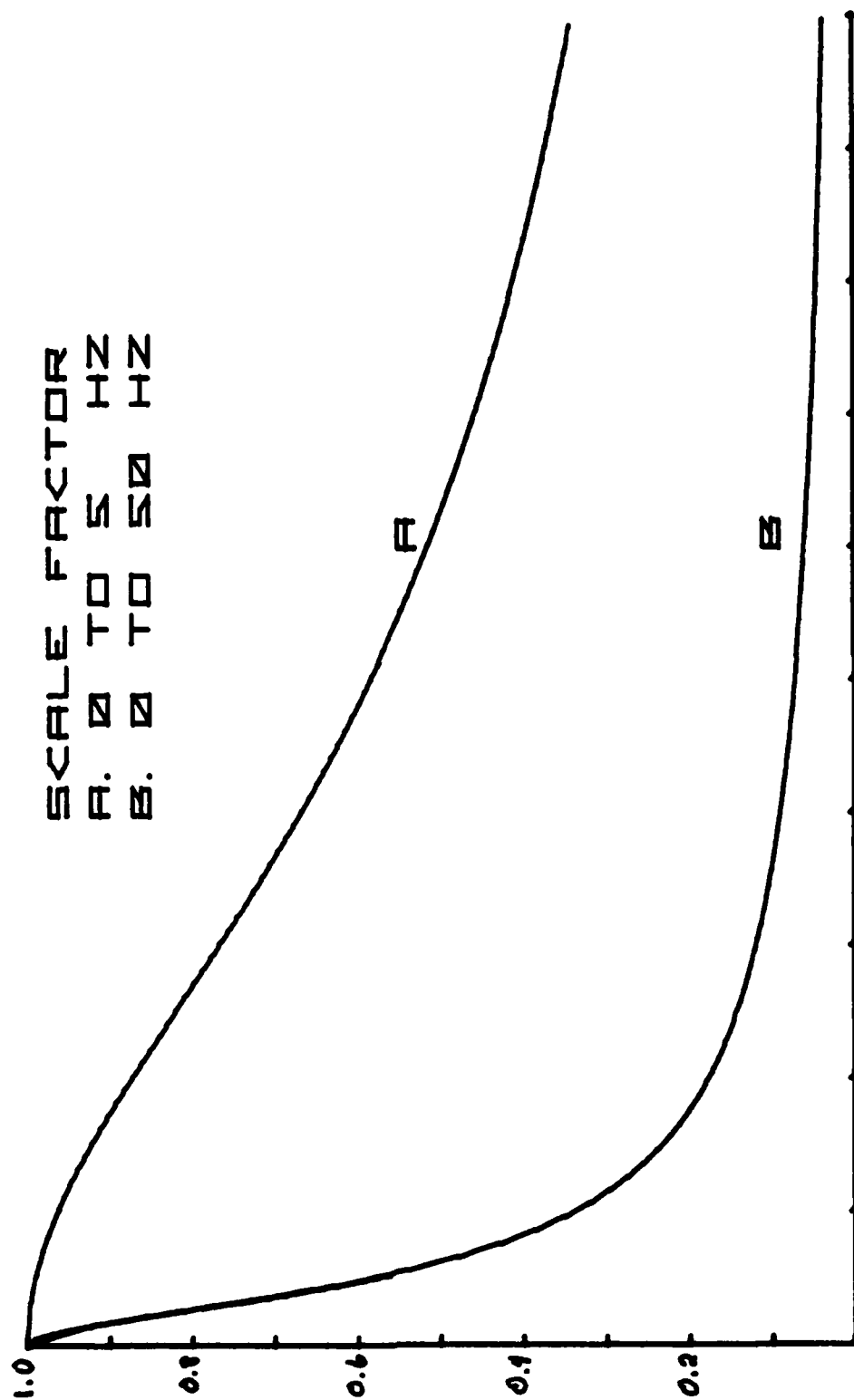
---

[4]Ibid.

Figure 1. Scaling Factor

17

"propagation" of the magnetic wave is the continuous generation

of it by the propagating acoustic wave.

III.   THE EXPERIMENT

A.   EXPERIMENTAL EQUIPMENT

The primary constraint on a laboratory experiment is space.
This shifts the operating frequency considerably above the
optimal range of the magneto-acoustic coupling as discussed
in the previous section, since the reduced dimensions cannot
contain the ULF acoustic wavelengths. A resonant cavity was
selected to contain the acoustic wave for two reasons. First,
it allows one to artificially produce long wavelengths in the
cavity instead of dealing with the free-space wavelength, as
would be the case for a pulsed source. Second, use of a
sinusoidally-varying acoustic source will induce a sinusoidally-
varying output signal in the presence of a DC magnetic field.
This facilitates signal processing for detection of the output
by permitting long integration times of the stable AC signal.

Because of the difficulty of achieving rigid boundaries
in an enclosure for a liquid, especially with the constraint
of non-magnetic construction required for this experiment,
pressure-release boundary conditions were selected. However,
this further increases the operating frequency for the experi-
ment, since the lowest mode that will fit into a pressure-
release cavity is the (1,1,1) mode (one half wavelength in
each dimension, x, y, and z), whereas a (0,1,0) mode would
fit into an identical but rigid enclosure. This shift in
frequency away from the region of efficient coupling requires

increasing the amplitude of the acoustic and magnetic fields
and the conductivity of the solution in order to achieve
measureable signal levels.

A Varian magnet, capable of stable magnetic fields on the
order of 0.7 Telsa with a $5\frac{1}{2}$ inch pole gap, was selected as
the source for the magnetic field. The overall configuration
of the magnet constrained the cross-section of the acoustic
tank to be approximately 0.1 by 0.3 meters. Plexiglass was
selected as material for construction of the tank because it
closely approximates a pressure-release surface on the exterior
walls of the tank, it is relatively easy to fabricate, and it
is non-magnetic. To simplify analysis of the acoustic wave,
the tank was constructed as a rectangular cavity 0.1 by 1.5 by
0.17 meters (inside dimensions).

The acoustic source for the experiment was a cylindrical
transducer, 0.15 meters in diameter. This transducer was
obtained on loan from Naval Ocean Systems Center, San Diego,
and it is capable of quite high source levels in the frequency
range of the experiment. However, the cylindrical source
necessitated construction of a cylindrical source cavity, to
be connected along its radius with one end of the rectangular
test cavity, in order to couple the radiated sound energy
effectively into the region of the magnetic field (see Figure 2).
Although optimal mutual resonance of the two cavities was never
achieved for the modal solution sought, an acceptable resonant
wave pattern was obtained in the far end of the test cavity.

Test Cavity

A. Side View

Test Cavity
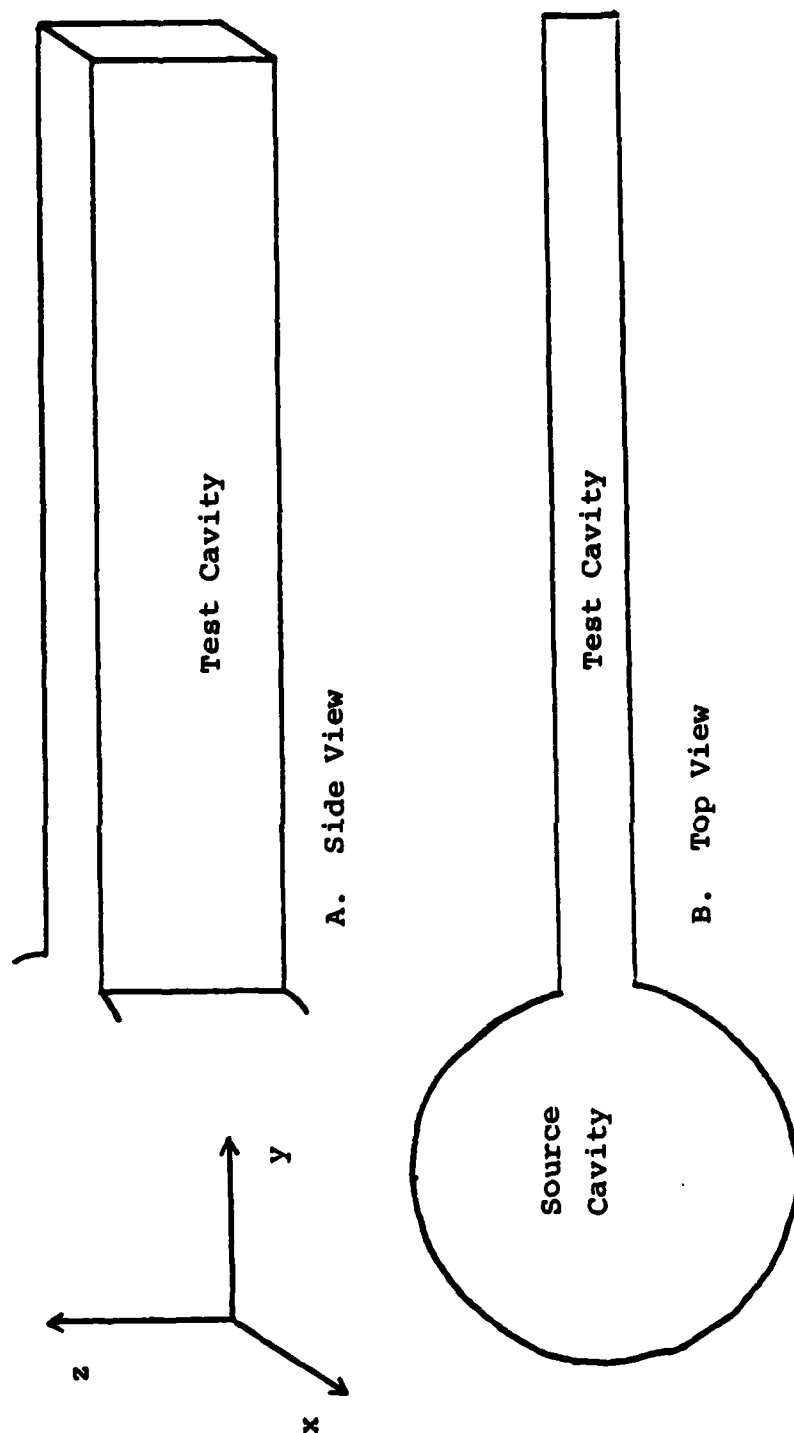
Source
Cavity

B. Top View

Figure 2. The Acoustic Wave Tank

A standing wave ratio of greater than ten-to-one was achieved with a half wavelength of about 0.305 meters. This acoustic field proved to be adequate for the experiment; see Appendix B for actual values achieved.

It was desired to obtain a low-order mode in the test tank; the first mode in the x and z dimensions (see Figure 3) for symmetry to facilitate analysis, and a half wavelength of greater than 0.3 meters in the y dimension in order to establish a uniformly polarized field within the influence of the magnet. The mode used for the experiment was a (1,5,1) mode (one half wavelength in the x and z dimensions and five half wavelengths in the y dimension) at about 10,350 Hz in salt water. This mode fulfilled the requirements of large amplitude, clean wave pattern, and acceptable wave dimensions for the experiment.

To further emphasize the interaction, a highly conductive medium was desired. Sea-salt saturated water was selected as the medium for its availability, but the conductivity achieved was so high that it was difficult to measure accurately with available equipment. An estimate was obtained using a conductivity bridge and a decade potentiometer, which, when corrected by comparison with the reading obtained for a standard potassium chloride solution, indicated a conductivity of 25 siemens/ meter. The accuracy of this measurement was estimated at about ±20%.

The experimental apparatus was set up as follows: A long rectangular plexiglass tank was filled with salt-saturated
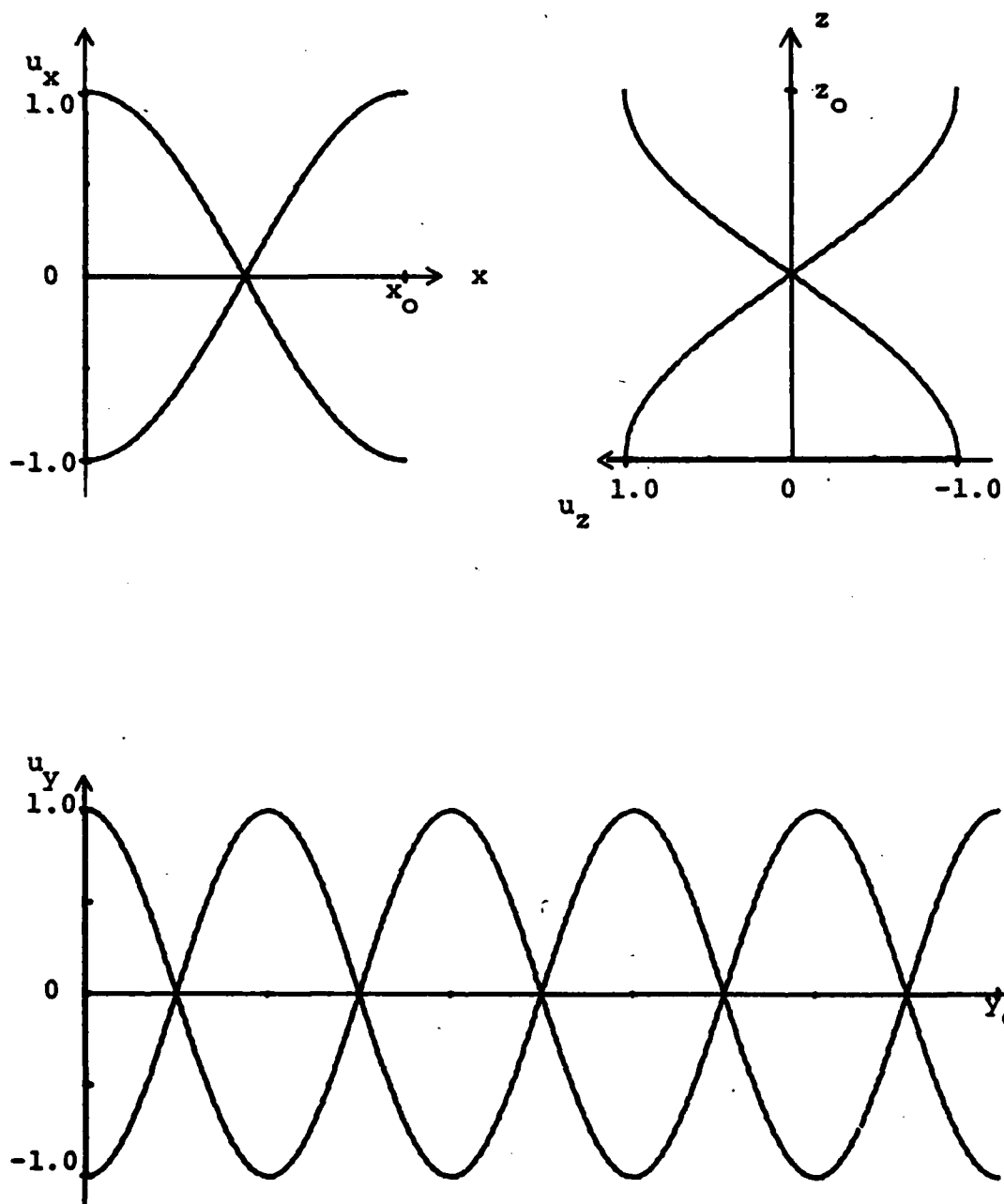
Figure 3. The Acoustic Standing Wave Patterns
for the Experimental Mode; Normalized
Velocity Amplitudes

23

water. An acoustic standing wave pattern was established in all three dimensions. A DC magnetic field was applied in the ±x direction across the tank, centered on a pressure node (and therefore a velocity anti-node) along the y dimension of the tank. Two copper-clad rectangular plates (0.1 by 0.3 meters) were placed at the surface and the bottom of the tank, centered longitudinally on the axis of the magnet, with leads attached to an amplifier and spectrum analyzer to detect any electric fields or current that were induced (see Appendix A and Figures 4 and 5).

B. EXPERIMENTAL ANALYSIS

With the equipment established as described in the previous section, measurements were initiated to establish a noise level. A large coherent noise component at the frequency of the acoustic wave was collected at the receiving plates, even in the absence of a magnetic field. Observation of this noise spike indicated it was pickup from the power leads to the transducer. The receiver plates functioned as a relatively efficient antenna for the strong fields created by the acoustic source equipment. Various shielding and grounding efforts reduced, but could not eliminate, the noise spike. However, the noise proved to be stable, coherent, and reproducible.

Upon introduction of the DC magnetic field, the induced signal adds to the noise spike coherently. By comparing the magnitudes of the magnet-free noise spike with the magnitudes of the signal-plus-noise output for the magnet polarized in
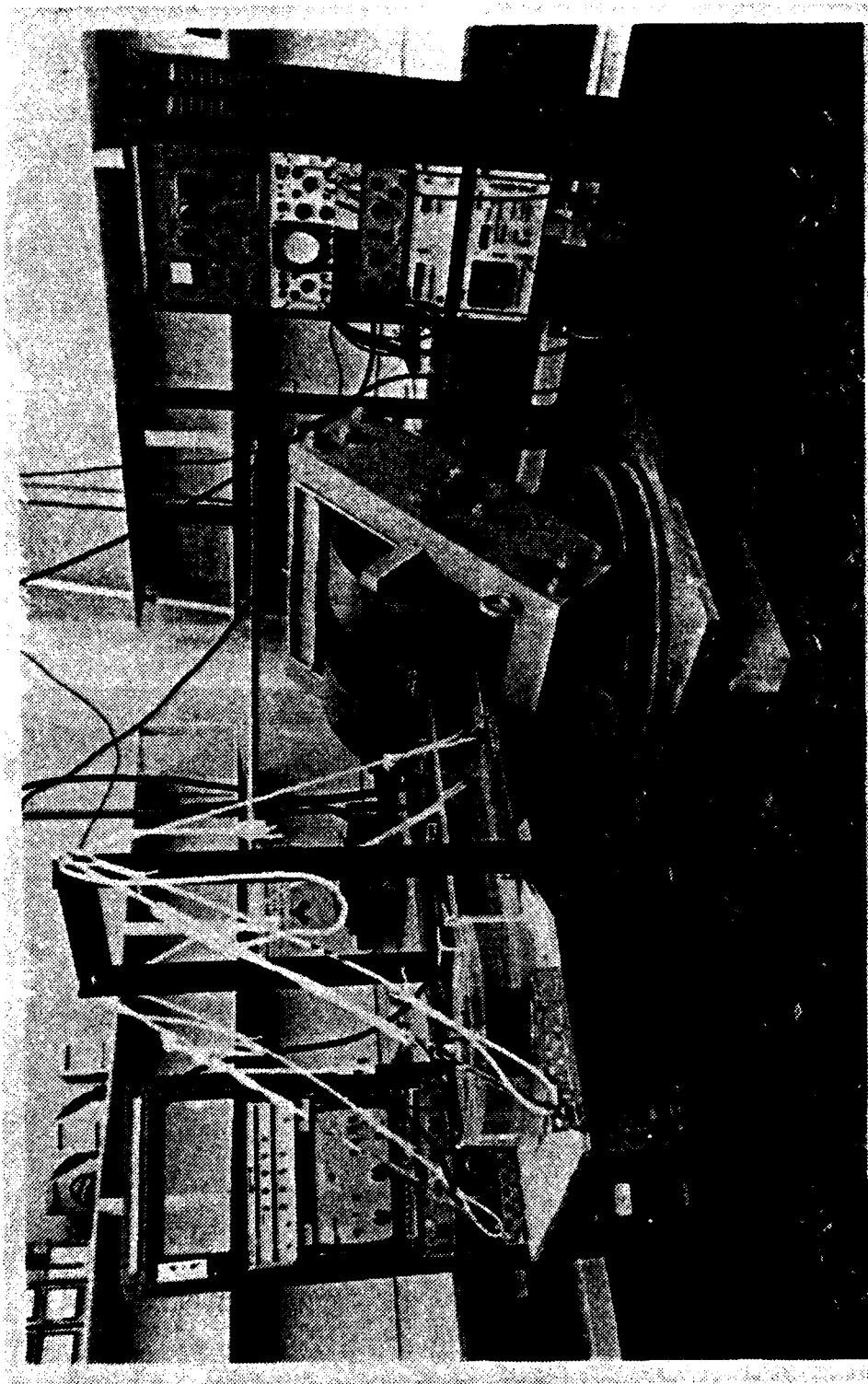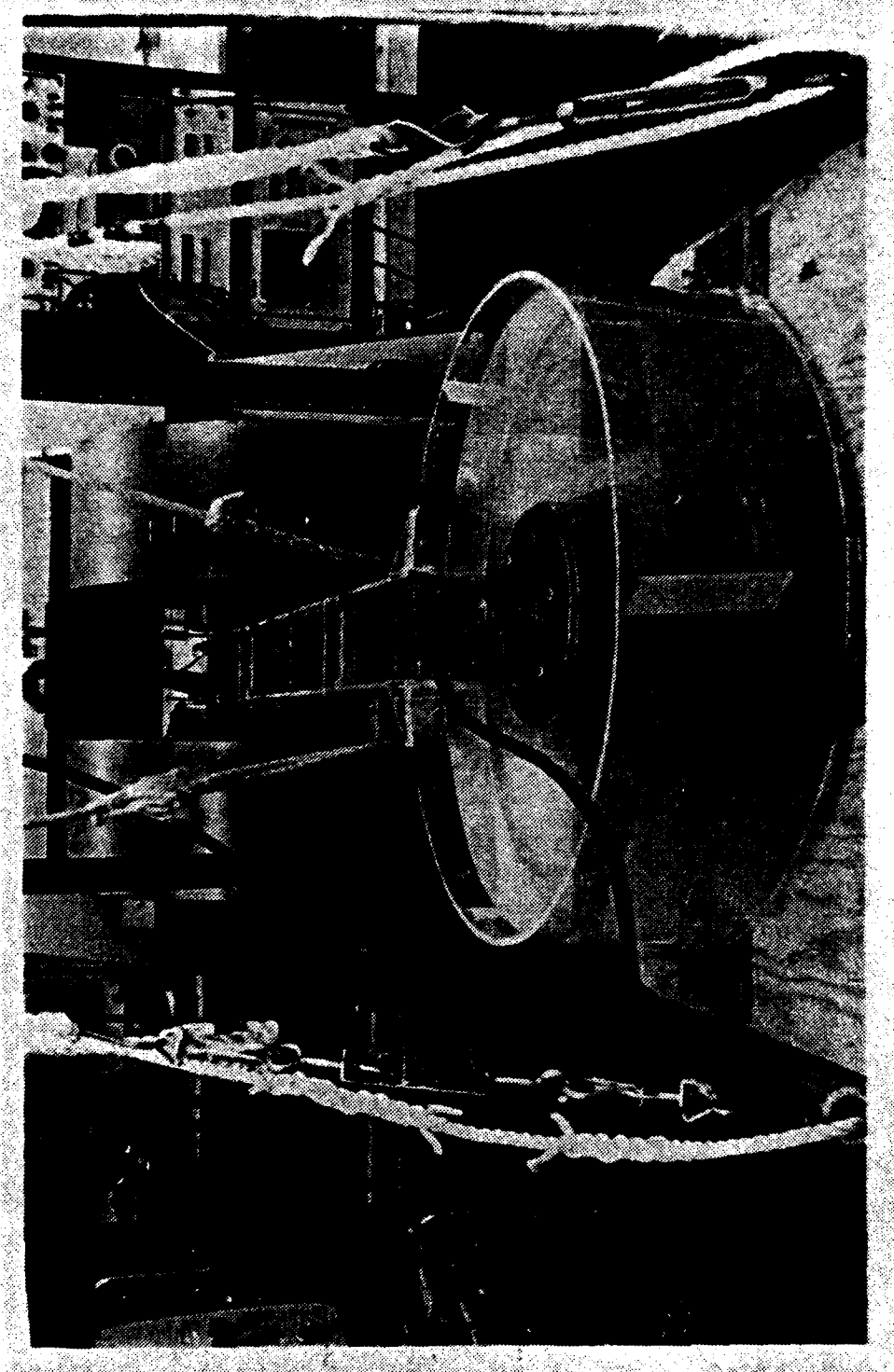
Figure 4. The Overall Experimental Apparatus

Figure 5. The Acoustic Tank Inside the Magnet

the "normal" and "reverse" modes, the magnitude of the induced
signal is obtained as follows: By observing that the noise
level is a consistent value, and that reversing the polarity
of the magnet shifts the phase of the induced signal by 180°
but does not affect its magnitude, two triangles with a
common side can be constructed in a phasor diagram as shown
in Figure 6.
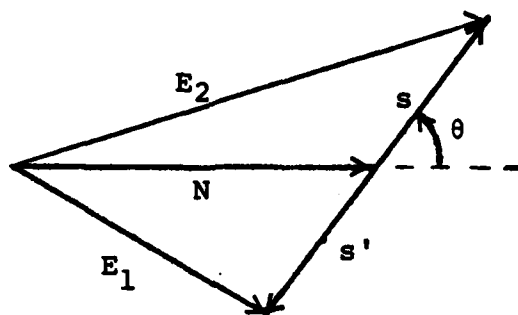

Figure 6. Phasor Resolution Diagram

The signal magnitude is then obtained by simultaneous
solution of the law of cosines for each triangle:

$$E_2^{\ 2} \ = \ N^2 + S^2 - (2\,N\,S)\ \cos(180-\theta)$$

$$(18)$$

$$E_1^{\ 2} \ = \ N^2 + S^2 - (2\,N\,S)\ \cos(\theta)$$

S and S' represent the signal phasors, N is the observed
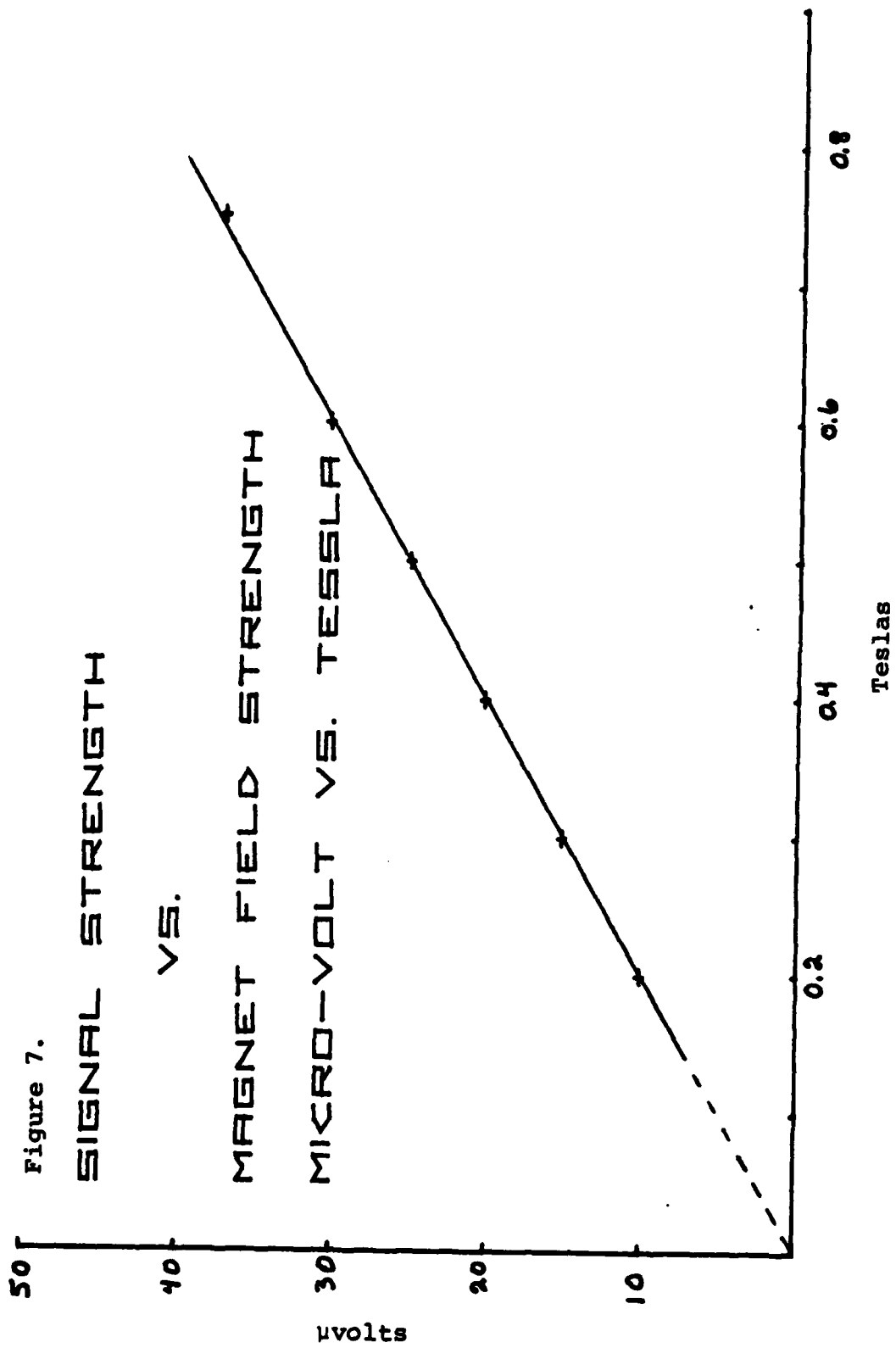noise phasor (assumed here with zero phase angle), and E_1

and E_2 represent the observed voltages with the magnetic field applied in either polarity.

Once resolved, the induced signal was found to vary linearly with the strength of the magnetic field, at constant acoustic amplitude, as predicted. Initial runs were made using a General Radio Audio Oscillator, which showed a slight frequency drift. Although this did not affect the acoustic resonance, the spectrum analyzer integrating the drifting output introduced about 15% data scatter into the results. This problem was resolved by shifting to a crystal frequency synthesizer (see Appendix A) and integrating the output signal for approximately three minutes for each data point. Several of these runs were then averaged for each value used in the above equations; the results are plotted in Figure 7. A remarkably linear variation of signal output with magnetic field strength at a rate of 50 μvolt/Tesla was observed.

In order to determine if the observed signal is, indeed, the postulated magneto-acoustic coupling, it is necessary to calculate the magnitude of the acoustic particle velocity. The wave equation for the acoustic velocity potential is

$$\nabla^2 \phi - \frac{1}{c_o^2} \frac{\partial^2 \phi}{\partial t^2} = 0 , \qquad (19)$$

where c_o is the mean sound velocity and, by definition, the acoustic velocity and pressure are given by

Figure 7.

SIGNAL STRENGTH

VS.

MAGNET FIELD STRENGTH

MICRO-VOLT VS. TESSLA

29

$$\bar{u} = \nabla \phi$$

(20)

$$p = - \rho_0 \frac{\partial \phi}{\partial t} .$$

ρ_0 is the average fluid density. From standard separation of variables and applying pressure-release boundary conditions, a solution is obtained of the form

$$\phi = \phi_0 \sin(k_x x) \sin(k_y y) \sin(k_z z) \qquad (21)$$

where

$$k_x = \frac{\ell \pi}{x_0} , \qquad k_y = \frac{m \pi}{y_0} , \qquad k_z = \frac{n \pi}{z_0} \quad (22)$$

are the associated wave numbers, and x_0, y_0, and z_0 are the effective cavity dimensions. Differentiation in the time domain introduces a factor of $i\omega$, so that

$$p = - \rho_0 \frac{\partial \phi}{\partial t} = - i \omega \rho_0 \phi \qquad (23)$$

or

$$\phi = \frac{i \, p}{\omega \, \rho_0} \qquad (24)$$

Using equations (19) above again yields

$$\bar{u} = \nabla \left[\frac{i|p|}{\omega \rho_o} \sin(k_x x) \sin(k_y y) \sin(k_z z) e^{i\omega t}\right]$$

$$= \frac{i|p|}{\omega \rho_o} e^{i\omega t} [k_x \sin(k_y y) \sin(k_z z) \cos(k_x x) \hat{i}$$

$$+ k_y \sin(k_x x) \sin(k_z z) \cos(k_y y) \hat{j} \tag{25}$$

$$+ k_z \sin(k_x x) \sin(k_y y) \cos(k_z z) \hat{k}]$$

The acoustic velocity field is of interest only insofar as it interacts with the magnetic field to produce a discernible signal, according to

$$\bar{E}_o = \bar{V} \times \bar{B} . \tag{26}$$

Since the magnetic field is uniquely polarized in the ±x direction, the cross-product with the x-component of the velocity field vanishes. Also, the z component will be a half wave cosine function at any point (in time and in the long dimension of the tank), and will therefore produce electrical components which are self-cancelling external to the tank. Therefore, the x and z components of the velocity field can be ignored for these calculations, and the relevant velocity field is reduced to

$$u_y = \frac{i|p|}{\omega \rho_o} k_y \sin(k_x x) \sin(k_z z) \cos(k_y y) e^{i\omega t}$$

$$\tag{27}$$

31

Incorporating the known dimensions and modal solutions for the experiment, and averaging the result over the effective x, y, and z dimensions for the effective strength yields

$$\langle u_y \rangle = 2.70 \frac{i|p|}{\omega \rho_o}$$

$$= 5.39 \times 10^{-5} \text{ meters/second} \tag{28}$$

from the observed parameters for the experiment, given in Appendix B.

To estimate the induced electric field strength of the magneto-acoustic interaction, couple this effective velocity magnitude with the DC magnetic field according to

$$\bar{E}_o = \bar{V} \times \bar{B} = u_y B \hat{k} \tag{29}$$

giving,

$$E_o = 53.9 \text{ } \mu\text{volt/meter/Tesla.}$$

This is equivalent, for the dimensions of the experiment, to an induced net voltage of $V_o = 7.50$ μvolt/Tesla, or about a factor of seven smaller than the observed signal voltage.

Another method of observing the magneto-acoustic coupling is to calculate the strength of the interaction as a current source. This approach attempts to compensate for leakage currents through the medium external to the source region.

Experimentally, this is accomplished by inserting known resistances R_s (shunt) in parallel with the receiver plates. From changes in output signal V_o with resistance, it is possible to calculate the apparent source strength I_o and leakage resistance R_1 by simultaneous solution from

$$I_o = \frac{V_o}{R_1} + \frac{V_o}{R_s} \qquad (30)$$

applied to several trials. This was carried out and the mean value of the induced apparent current source was approximately 400 μAmp/Tesla. For comparison, equation (25) can be rewritten

$$\bar{J}_o = \sigma \bar{V} \times \bar{B} \qquad (31)$$

or

$$I_o = (\sigma <u_y> B) \text{ (plate area)}$$

$$(32)$$

$$= 41.1 \text{ μAmp/Tesla,}$$

which is again about an order of magnitude smaller than the observed values.

Several experimental variations were attempted in an effort to explore the nature of the interaction and to verify that the observed signal was in fact the result of the phenomenon of magneto-acoustic coupling. The acoustic source level was

varied by set amounts, and the observed signal levels, with constant magnetic field, varied linearly. Also, the experiment was repeated in fresh water with several combinations of magnetic field phase and magnitude, with no discernible signal from the plates (this eliminates plate motion as a possible source of the excess observed signal level).

The experiment has established that an electric field is induced by the presence of an acoustic field in a conductive medium with a DC magnetic field for the geometry of this experiment. Despite the discrepancy between the magnitude of the signal observed and the calculated expected magnitude, a magneto-acoustic interaction is the probable cause of this induced signal.

IV. CONCLUSIONS AND DISCUSSION

In the first section it was demonstrated that an acoustic
wave propagating in a conductive medium in the presence of
a strong magnetic field should induce electric potential fields
and currents, and, associated with the electric currents, a
magnetic field. It was noted that the magnetic field arising
from the magneto-acoustic coupling should vary linearly with
the strength of the acoustic wave and the magnetic field, is
approximately inversely proportional to frequency, and is also
dependent on the strength of the medium parameters, e.g., the
sound velocity, permittivity, and conductivity. At ULF fre-
quencies in an actual ocean environment, these phenomena are
near the threshold of current detection capabilities and should
therefore be discernible in an appropriately low noise field.

In the second section, an experiment was reviewed in which
an electromagnetic signal was induced in a conductive salt
solution by the interaction of a DC magnetic field with a
resonant acoustic wave in a plexiglass cavity. The induced
signal responded in the same manner as the expected signal
from this coupling interaction, and its strength was within one
order of magnitude of an approximate calculation. It seems
reasonable to state on the basis of this evidence that the
basic interaction has now been verified in the laboratory.

There are a number of difficulties and questions left by this work, most evidently demonstrated in the disparity between experimental and theoretical magnitude.

Although the plexiglass cavity worked adequately for the experiment, as was remarked previously, it was still less than optimal. Significant difficulties were encountered in attempting to couple the two different geometry cavities together effectively. Most of the problem seems to be attributable to the impedance of the transducer face, an unknown in the design calculations. When mutual resonance of the two cavities was achieved (at higher frequencies and mode numbers that proved to be too short in wavelength for use in the experiment), an amplitude gain of 20 dB over the resonance mode used for the experiment was realized, along with higher standing wave ratios. The mode used for the experiment showed a good standing wave ratio and consistent sinusoidal wave patterns only at the end of the tank away from the source. The wave pattern in the region of coupling near the connection between the two cavities was muddled by evanescent modes. It is probable that a cleaner wave pattern would increase the sensitivity of the experiment considerably, and make the simplified Helmholtz solution used for the acoustic wave a more valid interpretation of experimental conditions.

Another area of compromise in the laboratory experiment was in the conductive fluid medium. Both the methods of mixing the salt solution and the methods of measuring the conductivity

of the result were limited to the materials and instruments on hand. The use of a pure salt (for example, sodium chloride or potassium chloride) would permit higher conductivities to be achieved and the conductivity of the result to be more consistent and predictable. Also, construction of a larger conductivity cell would enable more accurate measurements of a low-resistance solution than were possible with the instrumentation used for this experiment.
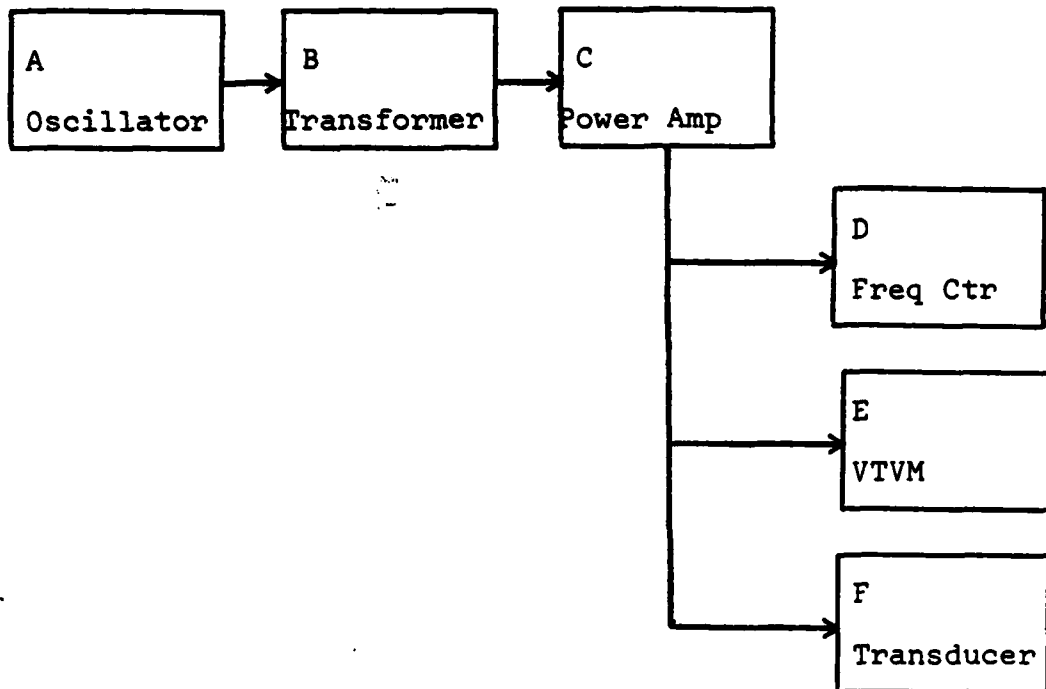
One other and more probable cause for the difference between the calculated and observed values of the induced currents is the method used to calculate the expected response. A more accurate potential function development for the fields occurring in and around the source region is necessary in order to precisely calculate the expected signal.

Another possible improvement on the experimental procedure would be to amplitude modulate the magnetic field sinusoidally, thereby inducing the magneto-acoustic signal at the sum and difference frequencies between the acoustic and magnetic frequencies. This would place the output away from the observed noise spike and remove any errors associated with the analysis of coherent addition between the signal and noise.
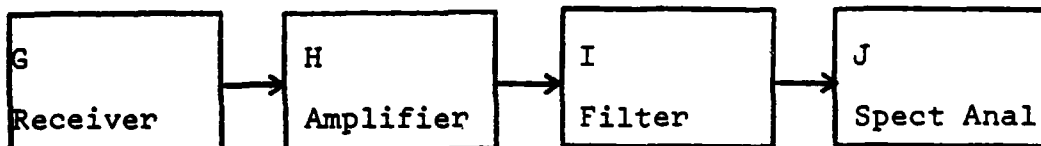
It is expected that further experimentation in this field will both confirm the results found here and expand the theory towards the goal of a practical application, as discussed in the Introduction.

APPENDIX A
Equipment Schematics

A	B	C
Oscillator	Transformer	Power Amp

D
Freq Ctr

E
VTVM

F
Transducer

Acoustic Source

G	H	I	J
Receiver	Amplifier	Filter	Spect Anal

Signal Reception

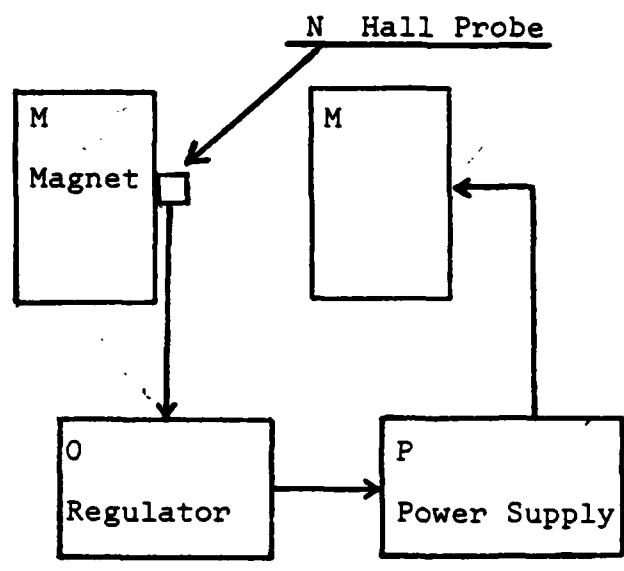| K	L
Hydrophone	O-Scope
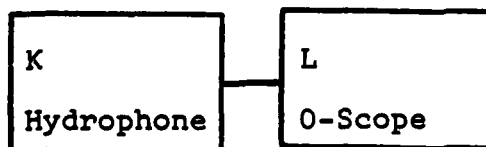
Acoustic Reception

38

Magnet Control

EQUIPMENT

A. Audio Oscillator
   Hewlett Packard Frequency Synthesizer, Model 3320B

B. Impedence Matching Transformer
   Krohn-Hite Matching Transformer, Model MT-56

C. Power Amplifier
   Krohn-Hite 50 Watt Amplifier, Model DCA-50

D. Frequency Counter
   Hewlett Packard Electronic Counter, Model 521C

E. VTVM
   Hewlett Packard Vacuum Tube Voltmeter, Model 400D

F. Transducer
   (NUSWC) B78CR8M

G. Receiver
   Copper-clad Fiberglass plates, 0.1 X 0.3 m

H. Voltage Amplifier
   Hewlett Packard Amplifier, Model 465A
   (set at +40 dB throughout experiment)

I. Filter
   Krohn-Hite Filter, Model 3750
   (settings: High-pass, 8,200 Hz cut-off, 18 dB/octave)

J. Specrum Analyzer
   EMR Schlumberger Digital Spectrum Analyzer, Model 1510
   EMR Schlumberger Digital Spectrum Translator, Model
   1520

K. Hydrophone
   Model LC-10 Transducer

L. Oscilloscope
   Tektronix Oscilloscope, Type RM 503

M. Magnet
   Varian Associates Electromagnet, Model V-4012-3B

N. Hall Effect Probe

O. Regulator
   Fielddial Magnetic Field Regulator, Model V-FR-2100

P. Magnet Power Supply
   Varian Associates Regulated Magnet Power Supply, Model
   V 2100 B

APPENDIX B

EXPERIMENTAL PARAMETERS

Test tank dimensions, in meters,

$$x_o = 0.1 \text{ meters}$$
$$y_o = 1.502 \text{ meters}$$
$$z_o = 0.139 \text{ meters}$$

Acoustic wave numbers (k_n) for the $(1,5,1)$ mode at $10,350$ Hz, in inverse meters,

$$k = 43.35$$
$$k_x = 31.42$$
$$k_y = 10.46$$
$$k_z = 22.60$$

Acoustic pressure amplitude, as measured with an LC-10 hydrophone with a sensitivity of -108.8 dB re 1 volt per microbar, in Pascals,

$$p = 2.15 \times 10^3$$
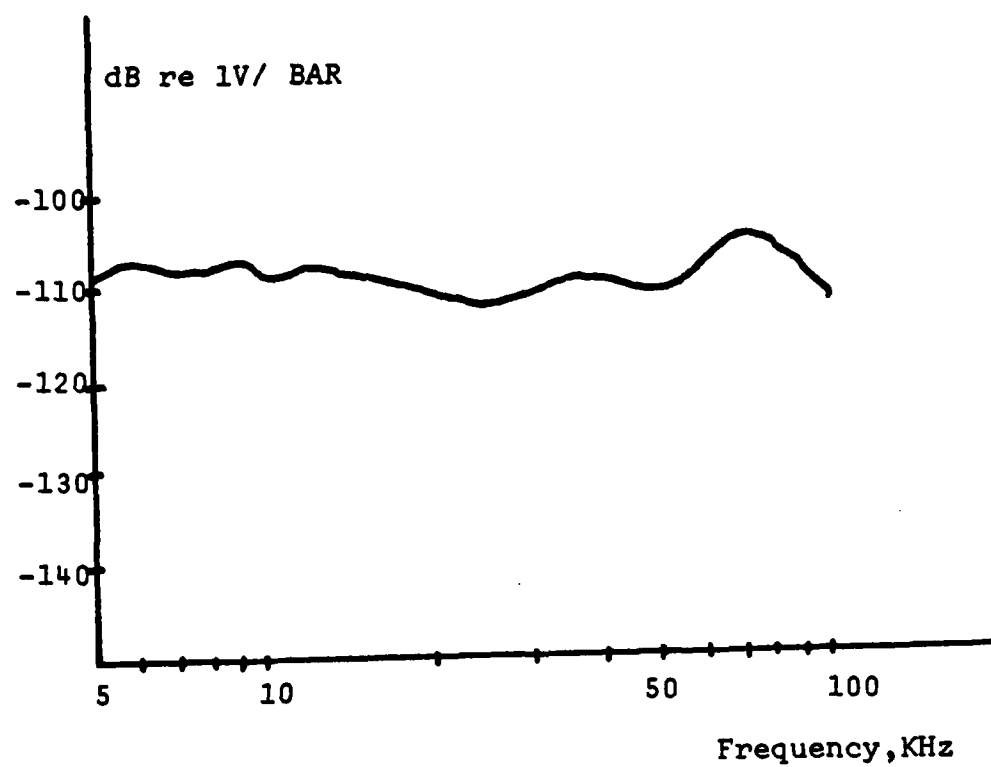$$p_{RMS} = 1.52 \times 10^3$$

Fluid Density

$$\rho_o = 1.17 \times 10^3 \text{ kg/m}^3$$

Fluid conductivity

$$\sigma = 25.4 \text{ siemens/meter}$$

APPENDIX C

Calibration Data

Sensitivity of the LC-10 Transducer, Serial No. 1922

Transmitting Response of the B78CR8M Transducer

BIBLIOGRAPHY

1. Anderson, Neal S., "Longitudinal Magneto Hydrodynamic Waves." <u>JASA</u>. May, 1953.

2. Kornhauser, E. T., "Magnetic Damping of Acoustic Waves in Conducting Media." <u>JASA</u>. 1953.

3. Bird, J. F., "Hydromagnetism Induced by Submerged Acoustic Sources: Sonomagnetic Pseudo Radiation." <u>JASA</u>. November, 1977.

INITIAL DISTRIBUTION LIST

		No. Copies
1.	Defense Documentation Center Building 5 Cameron Station Alexandria, VA 22314	2
2.	Library, Code 0142 Naval Postgraduate School Monterey, CA 93940	2
3.	Department Chairman, Code 61 Department of Physics Naval Postgraduate School Monterey, CA 93940	1
4.	Professor P. H. Moose, Code 61Me Department of Electrical Engineering Naval Postgraduate School Monterey, CA 93940	3
5.	LT. R. F. Klaus, USN NAVSUBSCOL SOAC Class 80-02 Groton, CT 06340	1
6.	Chief of Naval Research Department of the Navy 800 North Quincy Street Arlington, Virginia 22217	
	Code 100C1	1
	Code 460	1
	Code 463	5
	Code 480	1
7.	Commanding Officer Office of Naval Research Branch Office 1030 E. Green St. Pasadena, CA 91106	1
8.	Director Naval Research Laboratory Code 2627 Washington, D. C. 20375	6
9.	Office of Research, Development, Test, and Evaluation Department of the Navy Code NOP-987J Washington, D. C. 20350	1

10. Director   1
    Defense Advanced Research
    Projects Agency
    1400 Wilson Boulevard
    Arlington, Virginia 22209

11. Air Force Office of Scientific Research   1
    Department of the Air Force Directorate
      of Physics (MPG)
    Building 410
    Bolling Air Force Base
    Washington, D. C. 20332

12. Army Research Office   1
    Department of the Army
    Geosciences Division
    Box 12211
    Research Triangle Park, North Carolina 27709